PCCP

Accepted Manuscript

This article can be cited before page numbers have been issued, to do this please use: E. P. Månsson, S. De Camillis, M. C. Castrovilli, M. Galli, M. Nisoli, F. calegari and J. B. Greenwood, *Phys. Chem. Chem. Phys.*, 2017, DOI: 10.1039/C7CP02803B.

ROYAL SOCIETY OF CHEMISTRY

rsc.li/pccp

DOI: 10.1039/C7CP02803B

Ultrafast Dynamics in the DNA Building Blocks Thymidine and Thymine Initiated By Ionizing Radiation

E. P. Månsson[1], S. De Camillis[2], M. C. Castrovilli[1,4], M. Galli[1,3], M. Nisoli[1,3], F. Calegari[1,5], and J. B. Greenwood[2]

[1] Institute for Photonics and Nanotechnologies CNR-IFN, P.za Leonardo da Vinci 32, 20133 Milano, Italy

[2] Centre for Plasma Physics, School of Maths and Physics, Queen's University Belfast, BT7 1NN, UK

[3] Department of Physics, Politecnico di Milano, Piazza Leonardo da Vinci 32, 20133 Milano, Italy

[4] Inst. for the Structure of Matter CNR-ISM, Area della Ricerca di Roma 1, Monterotondo, Italy

[5] Center for Free-Electron Laser Science, DESY, Notkestr. 85, 22607 Hamburg, Germany

Abstract

Understanding of how energetic charged particles damage DNA is crucial for improving radiotherapy techniques such as hadron therapy and for the development of new radiosensitizer drugs. In the present study, the damage caused by energetic particles was simulated by measuring the action of extreme ultraviolet (XUV) attosecond pulses on the DNA building blocks thymine and thymidine. This allowed the ultrafast processes triggered by direct ionization to be probed with an optical pulse with a time resolution of a few femtoseconds. By measuring the yields of fragment ions as a function of the delay between the XUV pulse and the probe pulse, a number of transient processes typically lasting 100 femtoseconds or less were observed. These were particularly strong in thymidine which consists of the thymine base attached to a deoxyribose sugar. This dynamics was interpreted as excited states of the cation, formed by the XUV pulse, rapidly decaying via non-adiabatic coupling between electronic states. This provides the first experimental insight into the mechanisms which immediately proceed from the action of ionizing radiation on DNA and provides a basis on which further theoretical and experimental studies can be conducted.

View Article Online
DOI: 10.1039/C7CP02803B

Introduction

The response of DNA to ultraviolet and ionising radiation is critical in determining the necrosis and mutagenesis of cells. So a complete understanding of the mechanisms by which DNA reacts to different types of radiation is needed in order to develop new radiotherapy methods and improve radiation protection strategies. This is particularly relevant in aiding the development of hadron therapies and new radiosensitisers based on pharmaceuticals or nanoparticles. Extensive work has been undertaken using the bottom-up approach to study the influence of radiation on DNA building blocks in a variety of environments. This includes gas phase studies of the fundamental response of isolated molecules, which is particularly relevant for understanding the direct interaction mechanisms which dominate in high linear energy transfer radiotherapy.

There have been many gas phase studies of nucleobases, and to a lesser extent nucleosides, irradiated with ionising electromagnetic radiation, electrons, and heavy particles [1] [2] [3] [4] [5] [6] [7] [8] [9] [10] [11] [12] [13] [14] [15] [16]. Investigation of larger components of DNA are challenging due to the difficulty in vaporizing these large molecules, but a few experiments have been undertaken or are in development [17] [18] [19] [20]. Existing studies have mainly focussed on the ions produced, from which fragmentation pathways have been investigated and in some cases cross sections and appearance energies measured or calculated [21]. Recently, further understanding of the fragmentation mechanisms in these complex molecules has been obtained for the nucleoside thymidine using photoelectron-photoion coincidence (PEPICO) techniques in conjunction with theoretical calculations of the orbitals involved [22]. PEPICO allows the fragmentation spectrum to be matched to ionization of a specific orbital. The theoretical calculations show that the hole density created in the excited cation correlates with the fragments produced in terms of the subsequent bond breakages and charge location.

While the charge distribution in the molecule immediately after a sudden ionisation process is important to the resulting fragmentation, the ensuing dynamics in the molecule must also be playing a role. Indeed coherent charge oscillations in an amino acid following ionisation by an attosecond extreme ultraviolet pulse (XUV) has been recently observed [23] and the transfer of positive charge within DNA following oxidative damage is a key concept in understanding how strand breaks occur [24]. While the ultraviolet photo-protective properties of the neutral canonical nucleobases have been well studied using non-ionizing femtosecond pump-probe techniques [25] [26] [27], little work has been undertaken for ionising radiation. To perform similar experiments with ultrashort pulses of charged particles is difficult as fluxes are well below that achievable with laser pulses. However, by using broadband XUV attosecond pulses as the ionization source, equivalent studies with high temporal resolution can be undertaken. The analogy can be established by noting that if, for instance, a 500 eV electron or 1 MeV proton passes by a molecule, the component of the electric field experienced by the molecule resembles a single-cycle pulse with a large bandwidth. For an impact parameter of 0.2 nm (the diameter of the DNA helix) the spectrum of such a ‘pulse’ peaks around 10 eV and extends up to 100 eV.

The first measurements of the dynamics induced by ionisation with XUV pulses in molecules related to DNA were undertaken by Castrovilli et al. [28] in the radiosensitizers 5-fluoro- and 5-bromo-uracil. Near infrared-visible (NIR-VIS) pulses of 4 fs duration were used to probe changes in the fragment ion yields as a function of the delay between the two pulses. Strong changes in the yield of mass 43 and 44 u ions showed that a hydrogen atom could be transferred from the ring’s C6 to C5 site on a 35 fs timescale.

Another experiment with 5-fluoro-uracil was undertaken using femtosecond pump pulses consisting of the 3^{rd}, 5^{th} and 7^{th} harmonics of 400 nm, with the subsequent dynamics being probed with 800 nm pulses [29]. These results demonstrated that fragmentation of the molecule was influenced by ultrafast nonadiabatic processes, although this was complicated by additional dynamics of neutral Rydberg states excited by the 3^{rd} harmonic. Fast (30 fs) decay of cation states excited by the 5^{th}

View Article Online
DOI: 10.1039/C7CP02803B

harmonic was evident, along with delays (9 fs) in the probe absorption which indicated an even faster evolution of the excited populations.

In the present experiment attosecond pulses have been used to ionize an electron from a valence or sub-valence orbital of the nucleoside thymidine and nucleobase thymine. The molecules were then probed with a moderately intense 4 fs visible/near-infrared (VIS-NIR) pulse from which the ultrafast dynamics following ionization was investigated.

Methods

The ELYCHE attosecond beamline and the KEIRAlite mass spectrometer used for the experiments have been described in detail elsewhere [23] [30] [31] [32], but a brief description is provided here. The driving laser is a commercial Ti:Sapphire amplified laser (Femtopower PRO V CEP, Femtolaser), releasing 25-fs laser pulses with 6 mJ energy per pulse at 1 kHz repetition rate. The pulse bandwidth was widened by self-phase modulation through coupling of the laser beam to a 1 m hollow fiber with a helium gas gradient. After propagation through the fiber, the positively chirped pulse was compressed by chirped mirrors to a bandwidth limited pulse length of 4 fs with a pulse energy of 2.5 mJ and central wavelength of approximately 750 nm.

This few-cycle VIS-NIR laser beam was then divided by a broadband 70:30 split mirror into two components which constituted the pump and the probe arms for the time-resolved experiment. The pulse with the largest energy was focussed into a pulsed jet of krypton gas to produce XUV-pulses by high harmonic generation. The fundamental and low order harmonics were removed from the beam using a 100 μm thick aluminium filter and the attosecond beam was recombined with the probing VIS-NIR beam and focused with a 1 m focal length toroidal mirror into the interaction region of a time of flight mass spectrometer. The bandwidth of the XUV radiation spanned 17–40 eV as measured with a flat-field soft x-ray spectrometer. Temporally, the XUV radiation consisted of a short train of attosecond pulses lasting approximately 2 fs. The delay between the XUV and NIR pulses was controlled with attosecond precision using a delay stage actuated by a piezoelectric drive. Multiple scans were undertaken in alternating directions to account for any drift in the experimental conditions.

The gas phase target of the nucleobases and nucleosides was produced using a diode-laser induced thermal desorption source integrated into the repeller electrode of the KEIRAlite mass spectrometer which was operated in a time-of-flight mode. Solid samples of adenine, adenosine, thymine and thymidine were obtained from Sigma Aldrich (99%) and used without any further purification by applying them to a thin stainless foil which faced the interaction region. The intact, isolated, and neutral molecules were produced by irradiating the reverse side of the foil with a continuous wave diode laser. The exact temperature of the desorbed molecules is hard to determine accurately, but previous measurements taken under similar desorption conditions have shown that there is no fragmentation of any of the molecules prior to the interaction with the laser pulses [8] [33].

To quantify the pump-probe dynamics of individual fragments as function of probe delay, t, curves were fitted using either a prompt step with exponential decay, $f_1(t) = b + h \cdot e^{-(t-t_0)k}$, or an exponential change from an initial to a final level , $f_2(t) = b + h \cdot \left(1 - e^{-(t-t_0)k}\right)$. For $t < t_0$ both functions are defined equal to the baseline level, b. The parameter h is the step height, t_0 allows delayed steps and the rate constant, k, can be converted to a lifetime $\tau = 1/k$. For both models the underlying function is convoluted with a Gaussian to smoothen the step. The Gaussian full-width at half-max was held fixed at 11 fs. The two models can represent processes where the probe is absorbed either (1) from a short-lived state populated by the XUV pulse or (2) from an intermediate state reached after the initial decay. From here on, these fits are denoted as either model 1 or model 2, with positive or negative referring to the sign of h. The step height will be negative for ions

fragmented by the probe pulse while positive for daughter ions produced from the result of this interaction.

Results and Discussion

Figure 1 shows mass spectra obtained from ionization of thymine and thymidine by the XUV pulse. Thymine is a DNA base while thymidine is the corresponding nucleoside formed by bonding a deoxyribose sugar group to the N1 position of thymine. Given that the XUV pulse is able to singly ionize a wide range of molecular orbitals, it is not surprising that many different fragments can be produced and that the distribution has similarities to previous VUV, electron and ion impact spectra [3] [4] [6] [8] [9] [10] [33] [31]. The strongest contributions in the nucleoside correspond to breakage of the glycosidic bond between the base and sugar giving fragments with charge on the sugar (117 u) or on the base (126 u, requiring proton or H atom transfer). It is evident that when the thymidine and thymine spectra are compared, many of the lighter nucleoside fragments (99, 73, 45, 43, 31 u) do not appear in the nucleobase spectrum and can hence be associated with breakup of the sugar. The main fragment in the thymine spectrum, 55 u, also appears in the thymidine spectrum but this could also be derived from breakup of the sugar ring. Assignment of the main fragments in each spectrum is given in table 1.

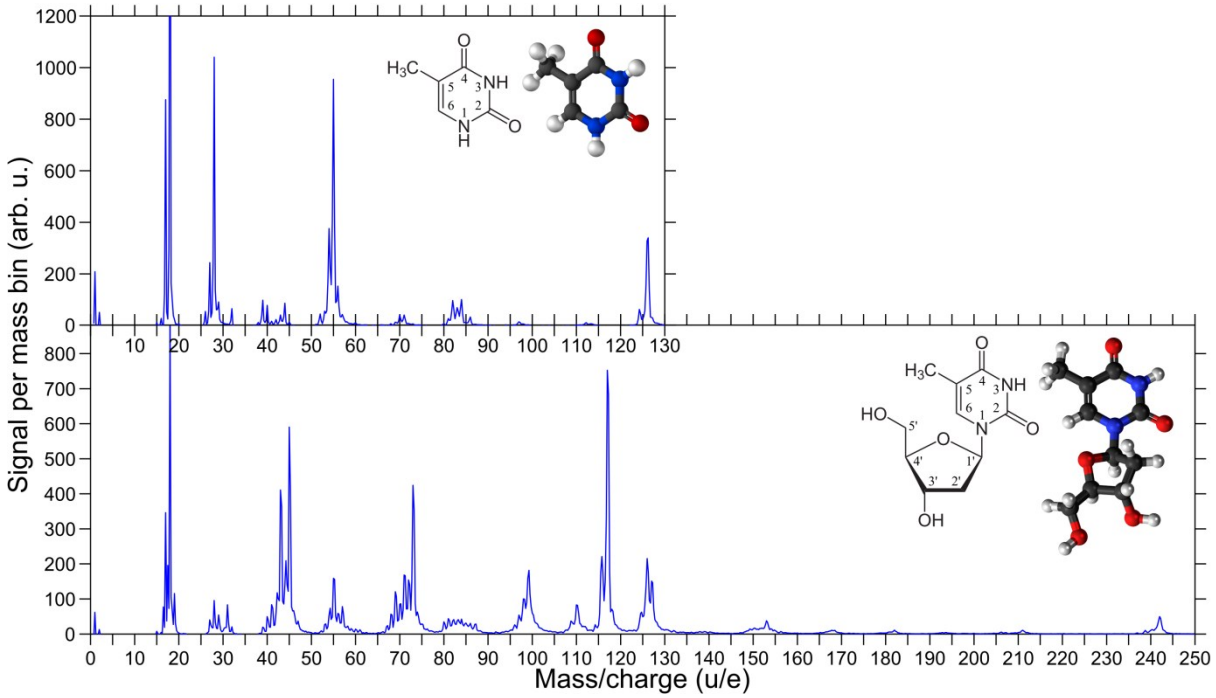

Figure 1: Mass spectra of thymine and thymidine irradiated with attosecond XUV pulses only.

Table 1: Main ions in thymine and thymidine mass spectra with chemical assignments associated with the deoxyribose sugar (S), thymine base (B) or residual gas (RG).

Mass (u)	Ion	Origin
15	CH_3 / NH	S / B
18	H_2O	RG
26	C_2H_2 / CN	S / B
27	C_2H_3 / CHN	S / B
28	C_2H_4 / CH_2N / N_2	S / B / RG
29	CHO / CH_3N	S / B
31	CH_3O	S

View Article Online
DOI: 10.1039/C7CP02803B

39	C_3H_3 / C_2HN	S / B
40	C_3H_4 / C_2H_2N	S / B
41	C_2HO / C_2H_3N	S / B
43	C_2H_3O / $CHNO$	S / B
44	C_2H_4O / CH_2NO	S / B
45	C_2H_5O	S
54	C_3H_4N	B
55	C_3H_3O / C_3H_5N	S / B
57	C_3H_5O	S
69	C_4H_5O	S
70	C_4H_6O / C_3H_4NO	S / B
71	C_4H_7O / C_3H_5NO	S / B
73	$C_3H_5O_2$	S
82	C_4H_4NO	B
83	C_4H_5NO	B
84	C_4H_6NO	B
99	S – H_2O	S
110	B – O / B – NH_2	B
117	S	S
125	B – H	B
126	B	B
127	B + H	B
153	B + C_2H_3	B + S
242	Thymidine	B + S

Maclot et al. [22] indicated that localization of the charge depends on the initial orbital ionized which in turn leads to different fragmentation channels. High charge density localised in the sugar part of the molecules for these excited cation states may explain the prevalence of sugar fragments in the mass spectrum, but ultrafast dynamics such as charge transfer towards the sugar side may also play a role.

The yields of selected thymidine fragments as a function of pump-probe delay are shown in Figure 2. It is evident that the time delay behaviour of most small fragments (masses 15, 27, 31, 39 u in Fig 2c) corresponds to model 1 positive (a sharp increase at time zero followed by an exponential decay), at the expense of the parent, sugar, and base ions (Fig 2a) all of which are reduced for positive probe delays. The size of steps shown in Fig 2c increased more strongly with probe pulse intensity than would be expected for a one photon process. Considering that breaking an additional bond often requires more than the 1.4–2.0 eV available from a probe photon, this suggests that many of the observed changes in the mass spectra result from absorption of two probe photons after XUV ionization.

The small ionic fragments in Figure 2c have low baseline levels and are best fitted by positive step functions with a decay (model 1). The shortest time constants of around 80 fs are found for the 15 u and 39 u fragments (see Table 2 for confidence intervals), while 31 u and 27 u decay more slowly (120 and 210 fs). For the parent (242 u) and sugar ions (117 u) which are described by model 2 negative, the initial states formed by the pump appear to have an even shorter lifetimes (20–30 fs), before they decay to intermediate states which are more accessible to probe absorption. These lifetimes should be considered with some caution as they do not refer to an exponential decay of the entire population but only for the portion expressed by the step-height parameter.

View Article Online
DOI: 10.1039/C7CP02803B

It is noted that the base (with zero, one or two hydrogens transferred from the sugar: 125, 126, 127 u), and the medium-sized fragments 99 u (the sugar having ejected neutral H_2O) and 73 u, are described by model 1 negative. This curve shape means that after the excitation by the XUV pulse the probe is only able to deposit energy in a limited time-interval to cause further fragmentation of these ions. The molecular dynamics in the cation leads to states or geometries where the probe pulse can no longer have this effect. The accessible state's lifetime was about 200 fs for the base and 99 u (the latter more uncertain) but only 40 fs for 73 u.

Figure 2b contains two small fragments (41 and 55 u) with baseline yields higher than fragments of similar mass in Figure 1. We can assume that these fragments have low appearance energies but still require breakage of at least 2 bonds. These fragments are described by model 2 positive indicating that the probe has no effect on the XUV-populated state, but a fast transition (20–50 fs lifetime) into a second excited state is able to enhance the observed fragment. The fitted lifetime for each fragment discussed is given in Table 2 together with confidence intervals.

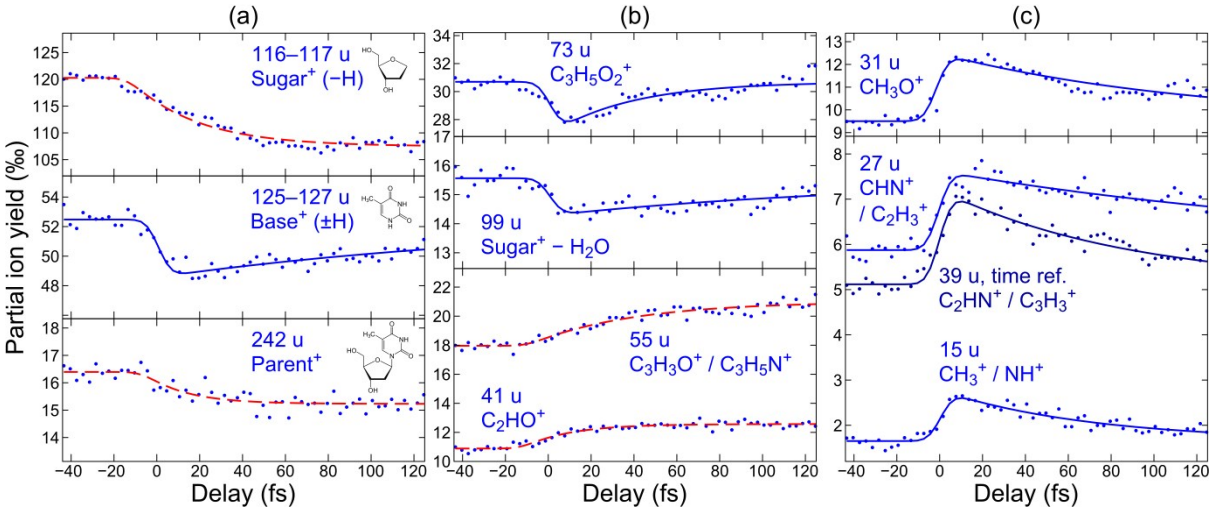

Figure 2: Ion yields obtained from thymidine as a function of pump-probe delay grouped according to: (a) most abundant ions in the spectrum corresponding to the parent, base and sugar ions; (b) fragment ions requiring two bond breakages but still prominent in the mass spectrum; (c) weaker ions corresponding to more complete fragmentation channels. The mass spectra were normalised to a total yield of 1000 and the partial ion yield axes give the relative contribution from each ion. The The data has been fitted as described in the text as solid blue lines for prompt steps (model 1), while gradual changes (model 2) are shown in dashed red. The delay scale uses the fragment 39 u step as time reference. The data points show the average from three consecutive scans.

With thymine as the sample, the pump–probe scan shows much less dynamics than thymidine. The fragment ions which exhibited a dependence on the pump-probe delay are shown in Figure 3. However, the steps in the yields at time zero are quite weak suggesting that for thymidine the strongest or most most easily probed dynamics upon XUV ionization occurs in the sugar of the nucleoside. Thymine fragments with masses 26, and 54/55 u are described by model 1 positive and negative respectively and have lifetimes of around 60 fs. The parent ion (126 u) is fitted using model 2 negative and has a similar lifetime (with larger uncertainty). However, for the 41 and 43 u fragments the lifetime is greater than 200 fs (model 1 positive). Confidence intervals for the thymine lifetimes are given in Table 2.

View Article Online
DOI: 10.1039/C7CP02803B

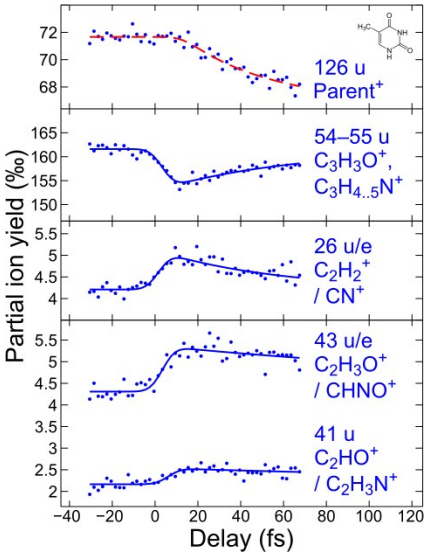

Figure 3: Yields of thymine and selected fragment ions as a function of pump-probe delay. The data points show the average from six consequtive scans.

Table 2: Fitted lifetimes of the thymidine and thymine ions in Figures 2 and 3. Approximate 68% confidence intervals are given within parentheses, obtained as the most extreme of (i) uncertainty in the shown curve fit and (ii) the mean ± standard deviation of fits to a few scans. An asterisk * indicates where model 2 has been used to fit the data.

Mass (u)	Thymidine Ion	Lifetime (fs)	
15	CH_3 / NH	70	(60–90)
27	C_2H_3 / CHN	210	(130–280)
31	CH_3O	120	(60–150)
39	C_3H_3 / C_2HN	90	(70–120)
41	C_2HO	20*	(15–35)
55	C_3H_5N / C_3H_3O	50*	(20–80)
73	$C_3H_5O_2$	40	(30–80)
99	S − H_2O	160	(110–800)
116–117	S (−H)	30*	(25–40)
125–127	B ± H	190	(140–300)
242	Parent	20*	(10–90)

Mass (u)	Thymine Ion	Lifetime (fs)	
26	C_2H_2 / CN	60	(40–90)
41	C_2HO	240	(40–∞)
43	C_2H_3O	220	(110–∞)
55	C_3H_5N / C_3H_3O	60	(30–90)
126	Parent	40*	(20–∞)

Given the complexity of these two molecules, there is probably a range of dynamical processes involved which cannot be individually identified without extensive theoretical work. However, the timescales we observe are consistent with fast nuclear movement on a potential energy surface leading to internal conversion into another electronic state. These transitions leads to a change in the probability of absorption of two probe photons. As can be seen for thymidine in Figure 1, in the absence of the probe pulse, breakage of the glycosidic bond producing the base or sugar cation is favoured. Figure 2 shows that delayed action of the probe can induce further bond breakages in the sugar which reduces the yield of 117u (model 2 negative), but increases the yields of fragments 41 u and 55 u (model 2 positive). It seems that while yields of these intermediate mass fragments are being generated from break-up of heavier ions, this increase is to a degree being balanced by losses through the formation of lower mass ions. These lighter fragments (27, 31, 39 u) are considerably weaker in the mass spectrum (lower baselines in the pump-probe scan) and therefore perhaps are derived from removal of an electron from a more strongly bound orbital which upon further

View Article Online
DOI: 10.1039/C7CP02803B

excitation by the probe results in multiple bond breakages. The 31 u fragment is the exception as it can be produced from a single bond breakage of CH_2OH from the sugar ring and has been calculated to be only 3 eV above the cation ground state [22]. So the observed time dependence may be due to an alternative channel arising from substantial breakup of the sugar ring.

Conclusion

This work is the first time-dependent study of the ultrafast dynamics induced in canonical DNA building blocks following sudden ionization. Sub-2fs XUV pulses were used to simulate energetic charge particle interactions and provide an accurate timestamp of the ionization event. A 4 fs NIR-VIS pulse was used to probe the subsequent dynamics by inducing additional bond breakages in the molecule through the absorption of additional photons. Ultrafast processes were observed through changes in the mass spectrum of the fragment ions produced.

For the nucleoside, thymidine, strong changes in the mass spectrum were induced by the probe pulse while in the nucleobase, thymine, only relatively weak modifications were observed. This suggests that absorption of the probe and the observable dynamics is concentrated in the sugar part of the molecule. For positive pump-probe delays, thymidine showed an enhancement in the yield of smaller fragments (15, 27, 31, 39 u), which reduced on timescales of less than 200 fs. This non-adiabatic dynamics in excited cation states reduced the probability of absorption of the probe as the molecular structure relaxed. Yields of more prominent fragments in the nucleoside mass spectra (41, 55 u) also grow for positive time delays but without an immediate increase at time zero and on faster timescales (< 50 fs). The fitted lifetimes suggest that a fast transition between excited cation states occurs, resulting in fragment enhancement through absorption of the probe. These gains appear to be at the expense of yields in parent and sugar ions which reduce on similar timescales. However, the single time constants fitted to each fragment yield is not reflective of a single process being present in each case. Given the bandwidth of the attosecond pulse, there are undoubtedly many electronic states contributing to the observed dynamics and unravelling these contributions is beyond the capability of the present set-up.

In a number of previous studies the clearest signature of this ultrafast non-adiabatic molecular dynamics in complex molecules has been found in the yields of doubly charged ions, where similar ultrafast transients have been found to be very common [29] [30] [32] [34] [35]. Although double ionization is likely to have occured in the present measurements, no stable dications were identified and the total number of ions created showed no significant dependence upon pump–probe delay. For future experiments, coincidence or covariance analysis of the singly charged ions would allow double ionization channels to be identified, even after dissociation into two singly-charged fragments, so that ultrafast processes such as charge migration could also be studied. The use of ultrashort ultraviolet pulses as a probe and/or pump could also increase the experimental time resolution and enable more site-specific excitation or ionization.

Ultimately to unravel the complex dynamics in these molecules will require substantial input from theoretical models which are able to simulate non-adiabatic coupling of the nuclear and electronic motion. While implementation is presently beyond present state-of-the-art, there are computer codes currently in development which will support experiments in the near future [36] [37] [38] [39] [40] [41] [42] [43]. This will be a huge step in developing a fuller understanding of the processes initiated by oxidative damage in DNA from ionizing radiation.

Acknowledgements

The authors acknowledge support by the ERC Starting Research Grant STARLIGHT No. 637756, ERC Research Grant ELYCHE No. 227355, the ‘‘Laserlab-Europe’’ Integrated Infrastructure Initiative

Contract No. CUSBO002011, the EU COST Actions CM1204 XLIC and CM1405 MOLIM, the Leverhulme Trust (RPG-2012-735), and EPSRC (EP/M001644/1).

View Article Online
DOI: 10.1039/C7CP02803B

References

[1] P. Bolognesi and L. Avaldi, in *Nanoscale Insights into Ion-Beam Cancer Therapy*, Springer, 2017, pp. 209-235.

[2] A. Giuliani, A. R. Milosavljević, F. Canon and L. Nahon, *Mass Spectrom. Rev.,* 2013, **33**, 424-441.

[3] E. Itälä, M. A. Huels, E. Rachlew, K. Kooser, T. Hägerth and E. Kukk, *J. Phys. B: At. Mol. Opt. Phys.,* 2013, **46**, 215102.

[4] H.-W. Jochims, M. Schwell, H. Baumgärtel and S. Leach, *Chem. Phys.,* 2005, **314**, 263–282.

[5] H. Levola, K. Kooser, E. Rachlew, E. Nõmmiste and E. Kukk, *Int. J. Mass Spectrom.,* 2013, **353**, 7-11.

[6] H. Levola, K. Kooser, E. Itälä and E. Kukk, *Int. J. Mass Spectrom.,* 2014, **370**, 96–100.

[7] S. Pilling, A. F. Lago, L. H. Coutinho, R. B. de Castilho, G. G. B. de Souza and A. Naves de Brito, *Rap. Comm. Mass Spectrom.,* 2007, **21**, 3646–3652.

[8] J.-C. Poully, J. Miles, S. De Camillis, A. Cassimi and J. B. Greenwood, *Phys. Chem. Chem. Phys.,* 2015, **17**, 7172-7180.

[9] S. Ptasińska, P. Candori, S. Denifl, S. Yoon, V. Grill, P. Scheier and T. D. Märk, *Chem. Phys. Lett.,* 2005, **409**, 270–276.

[10] P. J. M. van der Burgt, F. Mahon, G. Barrett and M. L. Gradziel, *Eur. Phys. J. D,* 2014, **68**, 151.

[11] P. J. M. van der Burgt, S. Finnegan and S. Eden, *Eur. Phys. J. D,* 2015, **69**, 173.

[12] P. Rousseau and B. A. Huber, in *Nanoscale Insights into Ion-Beam Cancer Therapy*, Springer, 2017, pp. 121-157.

[13] J. Tabet, S. Eden, S. Feil, H. Abdoul-Carime, B. Farizon, M. Farizon, S. Ouaskit and T. D. Märk, *Int. J. Mass Spectrom.,* 2010, **292**, 53–63.

[14] T. Schlathölter, F. Alvarado, S. Bari, A. Lecointre, R. Hoekstra, V. Bernigaud, B. Manil, J. Rangama and B. Huber, *ChemPhysChem,* 2006, **7**, 2339–2345.

[15] I. Miranda-Santos, S. Gramacho, M. Pineiro, K. Martinez-Gomez, M. Fritz, K. Hollemeyer, A. Salvador and E. Heinzle, *Anal. Chem.,* 2015, **87**, 617–623.

[16] P. Markush, P. Bolognesi, A. Cartoni, P. Rousseau, S. Maclot, R. Delaunay, A. Domaracka, J. Kocisek, M. C. Castrovilli, B. A. Huber and L. Avaldi, *Phys. Chem. Chem. Phys.,* 2016, **18**, 16721-16729.

View Article Online
DOI: 10.1039/C7CP02803B

[17] E. Dudley and L. Bond, *Mass Spectrom. Rev.,* 2014, **33**, 302–331.

[18] J. Duron and L. Hargreaves, *Bull. Am. Phys. Soc.,* 2016, vol. 61, no. 2.

[19] J.-W. Shin and E. R. Bernstein, *J. Chem. Phys.,* 2014, **140**, 044330.

[20] O. González-Magaña, M. Tiemens, G. Reitsma, L. Boschman, M. Door, S. Bari, P. O. Lahaie, J. R. Wagner, M. A. Huels, R. Hoekstra and T. Schlathőlter, *Phys. Rev. A,* 2013, **87**, 032702.

[21] M. C. Castrovilli, P. Bolognesi, A. Casavola, A. Cartoni, D. Catone, P. O'Keeffe and L. Avaldi, *Eur. Phys. J. D,* 2014, **68**, 253.

[22] S. Maclot, R. Delaunay, D. G. Piekarski, A. Domaracka, B. A. Huber, L. Adoui, F. Martín, M. Alcamí, L. Avaldi, P. Bolognesi, S. Díaz-Tendero and P. Rousseau, *Phys. Rev. Lett.,* 2016, **117**, 073201.

[23] F. Calegari, D. Ayuso, A. Trabattoni, L. Belshaw, S. De Camillis, S. Anumula, F. Frassetto, L. Poletto, A. Palacios, P. Decleva, J. B. Greenwood, F. Martín and M. Nisoli, *Science,* 2014, **346**, 336-339.

[24] A. Kumar and M. D. Sevilla, *Chem. Rev.,* 2010, **110**, 7002–7023.

[25] C. T. Middleton, K. de La Harpe, C. Su, Y. K. Law, C. E. Crespo-Hernández and B. Kohler, *Annu. Rev. Phys. Chem.,* 2009, **60**, 217-239.

[26] K. Kleinermanns, D. Nachtigallová and M. S. de Vries, *Int. Rev. Phys. Chem.,* 2013, **32**, 308–342.

[27] V. Stavros and J. R. R. Verlet, *Annu. Rev. Phys. Chem.,* 2016, **67**, 211-232.

[28] M. C. Castrovilli, A. Trabattoni, P. Bolognesi, P. O'Keeffe, L. Avaldi, M. Nisoli, F. Calegari and R. Cireasa, *J. Phys. Conf. Ser.,* 2015, **635**, 112131.

[29] P. Çarçabal, D. Descamps, S. Petit, Y. Mairesse, V. Blanchet and R. Cireasa, *Faraday Discuss.,* 2016, **194**, 407-425.

[30] F. Calegari, A. Trabattoni, A. Palacios, D. Ayuso, M. C. Castrovilli, J. B. Greenwood, P. Decleva, F. Martín and M. Nisoli, *J. Phys. B: At. Mol. Opt. Phys.,* 2016, **49**, 142001.

[31] C. R. Calvert, L. Belshaw, M. J. Duffy, O. Kelly, R. B. King, A. G. Smyth, T. J. Kelly, J. T. Costello, D. J. Timson, W. A. Bryan, T. Kierspel, P. Rice, I. C. E. Turcu, C. M. Cacho, E. Springate, I. D. Williams and J. B. Greenwood, *Phys. Chem. Chem. Phys.,* 2012, **14**, 6289–6297.

[32] L. Belshaw, F. Calegari, M. J. Duffy, A. Trabattoni, L. Poletto, M. Nisoli and J. B. Greenwood, *J. Phys. Chem. Lett.,* 2012, **3**, 3751−3754.

[33] S. De Camillis, J. Miles, G. Alexander, O. Ghafur, I. D. Williams, D. Townsend and J. B. Greenwood, *Phys. Chem. Chem. Phys.,* 2015, **17**, 23643-23650.

[34] A. Marciniak, V. Despré, T. Barillot, A. Rouzée, M. C. E. Galbraith, J. Klei, C. H. Yang, C. T. L. Smeenk, V. Loriot, S. N. Reddy, A. G. G. M. Tielans, S. Mahapatra, A. I. Kuleff, M. J. J. Vrakking and F. Lépine, *Nat. Comm.,* 2015, **6**, 7909.

[35] F. Calegari, D. Ayuso, A. Trabattoni, L. Belshaw, S. De Camillis, F. Frassetto, L. Poletto, A. Palacios, P. Decleva, J. B. Greenwood, F. Martín and M. Nisoli, *IEEE JSTQE,* 2015, **21**, 8700512.

[36] M. Lara-Astiaso, D. Ayuso, I. Tavernelli, P. Decleva, A. Palacios and F. Martín, *Faraday Discuss.,* 2016, **194**, 41-59.

[37] A. Wardlow and D. Dundas, *Phys. Rev. A,* 2016, **93**, 023428.

[38] K. E. Spinlove, M. Vacher, M. Bearpark, M. A. Robb and G. A. Worth, *Chem. Phys.,* 2017, **482**, 52-63.

[39] V. Despré, A. Marciniak, V. Loriot, M. C. E. Galbraith, A. Rouzée, M. J. J. Vrakking, F. Lépine and A. I. Kuleff, *J. Phys. Chem. Lett.,* 2015, **6**, 426-431.

[40] Z. Li, O. Vendrell and R. Santra, *Phys. Rev. Lett.,* 2015, **115**, 143002.

[41] S. Martin and M. Hochlaf, in *Photoinduced Phenomena in Nucleic Acids I*, Springer, 2014, pp. 155-208.

[42] D. Mendive-Tapia, M. Vacher, M. J. Bearpark and M. A. Robb, *J. Chem. Phys.,* 2013, **139**, 044110.

[43] M. Vacher, M. J. Bearpark, M. A. Robb and J. P. Malhado, *Phys. Rev. Lett.,* 2017, **118**, 083001.

J. Barker, in *Catalyst Deactivation*, ed. B. Delmon and C. Froment, Elsevier, Amsterdam, 2nd edn, 1987, vol. 1, ch. 4, pp. 253–255.